POLITECNICO DI TORINO
Repository ISTITUZIONALE

Functionalized polyamide membranes yield suppression of biofilm and planktonic bacteria while retaining flux and selectivity

Original
Functionalized polyamide membranes yield suppression of biofilm and planktonic bacteria while retaining flux and selectivity / Dadashi Firouzjaei, M.; Pejman, M.; Gh, M. S.; Aktij, S. A.; Zolghadr, E.; Rahimpour, A.; Sadrzadeh, M.; Shamsabadi, A. A.; Tiraferri, A.; Elliott, M.. - In: SEPARATION AND PURIFICATION TECHNOLOGY. - ISSN 1383-5866. - 282:(2022), p. 119981. [10.1016/j.seppur.2021.119981]

Availability:
This version is available at: 11583/2950993 since: 2022-01-18T14:54:42Z

Publisher:
Elsevier B.V.

Published
DOI:10.1016/j.seppur.2021.119981

Terms of use:

This article is made available under terms and conditions as specified in the corresponding bibliographic description in the repository

Publisher copyright

(Article begins on next page)

06 May 2026

ISSN 1590-8844
International Journal of Mechanics and Control, Vol. 25, No. 01, 2024

doi.org/10.69076/jomac.2024.0015

A COMPUTATIONAL METHODOLOGY FOR RECUMBENT BICYCLE FITTING TO OPTIMIZE AERODYNAMIC EFFICIENCY WHILE ENSURING RIDER COMFORT

Elisa Digo* Lorenzo Ingrosso** Manuela Vargas*** Cristina De Vito** Chiara Gastaldi*,**

* Politecnico di Torino, Department of Mechanical and Aerospace Engineering

** Politecnico di Torino, Policumbent Student Team

*** fleXstructures Italia Srl

ABSTRACT

This paper provides an overview of recent advancements in the field of bicycle fitting, focusing on the balance between aerodynamic advantages and physical performance. The importance of achieving optimal bicycle rider positioning is emphasized, particularly in enhancing performance and preventing pathology. The historical evolution of bicycle fitting methods, from subjective preferences to evidence-based approaches, is discussed, along with the role of technology in facilitating biomechanical analysis and simulation. The paper introduces a computational methodology (IPS IMMA software) for fitting a racing faired recumbent bicycle, emphasizing the need to integrate biomechanics and aerodynamics considerations. By aligning rider posture with biomechanical recommendations and minimizing encumbrance, the proposed methodology aims to enhance both aerodynamic efficiency and rider comfort. The article concludes with a presentation of methods and results, highlighting trends and ranges of motion during the pedalling cycle. Gender-based differences in joint angles are highlighted, thus underscoring the need for tailored fitting approaches.

Keywords: pedalling; recumbent bicycle; joint angle; computational methodology

1 INTRODUCTION

In today's society, an increasing number of people are incorporating regular exercise and sports into their daily routines to maintain their health and promote well-being at all ages [1,2]. Among the many possibilities of physical activity, riding a bicycle represents an effective cyclic exercise that produces positive effects in terms of fitness improvement and psychological well-being. Additionally, cycling can serve as an alternative mode of transportation for sustainable mobility [3].

A fundamental requirement for an optimal bicycle riding is to reach an appropriate balance between aerodynamic advantages and physical performance [4,5].

Contact author: Elisa Digo[1]

[1]Corso Duca degli Abruzzi, 24 – 10129 Torino, Italy
E-mail: elisa.digo@polito.it

Accordingly, one of the primary ways to maximize performance and comfort while preventing pathology is represented by bicycle fitting. In detail, it consists in a structured process based first on the evaluation of the cyclist's physical and performance requirements, then on the identification of the cyclist's goals and needs, and finally on the consequent systematic adjustment of the bike also considering the rider's anthropometric measures [6].

To obtain the optimal position of each cyclist, it is necessary to adjust the three interfaces between the human body and the bicycle: the shoe-cleat-pedal (i.e., cleat adjustment, horizontal distance between feet and crank arm length, pedal type), the pelvis-saddle (i.e., saddle height, type, and setback), and the hands-handlebar (i.e., handlebar model, length, and height) [6,7].

The first research on the correct positioning of bike elements for an optimal cyclist posture was not evidenced-based, but just determined on personal preference and opinion [8]. Subsequently, the advancement of technology allowed simulating or directly recording cyclists' 2D and 3D kinematics during riding. Literature works have already

approached the exercise of bicycle riding from a biomechanical and aerodynamical point of view, also considering the concept of bicycle fitting. Some works compared different bicycle positions such as upright, recumbent, and supine, determining the characteristics of maximum pedalling performance in terms of muscles strength, joint angles, body centre of mass, limb mechanical work, operative ranges of propulsive muscles, metabolic and ventilatory efficiency [9-11]. Moreover, Scoz et al. analysed riders' subjective responses in terms of pain level, discomfort, and fatigue to a standardized ergonomic adjustment of the bicycle [12]. Focusing on stationary cycling, the studies of Thorsen et al. [13] and Lu et al. [14] examined the effects of different horizontal distances between bike pedals, seat positions, or work rates on the knee biomechanics during upright and recumbent cycling, respectively. In addition, Yen et al. examined the recumbent exercise bicycles by adopting riders' subjective comfort levels to determine optimal seat positions for riding [1]. In the work of Momeni et al., the contribution and functioning of upper and lower leg muscles was evaluated during semi-reclined cycling at different workloads and constant cadence [15]. In stationary conditions, motion characteristics were compared between able-bodied and spinal cord injured subjects [16].

Two of the most influential biomechanical variables associated with the bike fitting and overuse injuries are the maximum knee flexion angle and the cyclist's degree of trunk flexion [17]. Literature suggests a recommended knee flexion angle to prevent injuries and optimize cycling efficiency while avoiding negative effects on trunk and lower legs [18]. To improve the aerodynamics and consequently to reduce the forces of resistance opposed to motion, a greater trunk inclination is guaranteed in the recumbent bicycle. However, the maintenance of this position over time can provoke neck and lower back pain, which can be explained through the viscoelastic structures and the mechanical creep of the spine due to the constant load [19]. Accordingly, it is necessary to find a good compromise among aerodynamics, performance, and health for the knee flexion and the trunk inclination during cycling. Faired recumbent bicycles, also known as velomobiles [20,21], are able to improve the aerodynamic performance thanks to the fairing. However, especially in racing prototypes, the space inside the fairing is limited, therefore finding a compromise between performance, comfort, and ergonomics is a challenging task.

Even if experimental methods are very effective in objectively studying and characterizing the movement, they can also be extremely time and resource consuming. Since computational methods guarantee the repeatability in ideal scenarios and the reduction of time and cost [22], they can be considered a suitable alternative to study the movement of the human and/or the environment with which human interacts in several contexts [23-25]. Such methods are especially relevant at the vehicle design stage, when the physical bicycle prototype is not yet available, but having an estimate of the cyclist interaction with the vehicle is necessary. Having a cyclist virtual prototype is paramount to ensure that the vehicle will interact optimally with its source of power, i.e. the rider, thus guaranteeing optimal performance. No structured approach for a racing faired recumbent bicycle is available in the literature. The aim of the present paper was to approach bicycle fitting of a racing faired recumbent bicycle through a computational methodology. The cyclist's encumbrance was estimated through a computational method, which allowed to simulate the riding of a biker with known anthropometric data, guaranteeing a proper balance between biomechanics and aerodynamics and hence finding the most effective ergonomic characteristics of the bicycle. Accordingly, aerodynamic requirements were here focused on minimizing the encumbrance of the rider-bike system in both the sagittal and the frontal planes. On the sagittal plane, this requirement was fulfilled aligning the head with the toes and the pelvis with the heels, hence forcing the knee flexion angle to be inside the range suggested by literature. On the frontal plane, the variation of joint angles was assumed equal to zero. Moreover, the head and the hips of the rider were considered still to maintain the riding position. Two simulations were conducted selecting a dummy of the 95th percentile male and a dummy of the 5th percentile female. During both simulations, angles of trunk, hip, knee, and ankle in the sagittal plane were saved every 5 degrees of the fourth riding cycling (selected as a steady-state condition).

The article is organized as follows. First, methods are presented focusing on the description of the IPS IMMA software, the execution of simulations, and the analysis of data. Then, the main results related to joint angular trends, ranges of motion, and minimum values during the pedalling cycle are presented and discussed.

2 METHODS

2.1 IPS IMMA SOFTWARE

Industrial Path Solutions (IPS) is a software house based on virtual algorithms to realize products. In detail, IPS tools are used by factories to verify the feasibility of assembly, to project flexible components, to optimize robotic tools, and to simulate procedures of superficial treatments [26].

IPS IMMA (Intelligently Moving Manikin) is a Digital Human Modelling (DHM) software endowed with advanced path-planning techniques that allows a digital representation of the human body and behaviour inside a simulation or a virtual environment to facilitate the analysis of safety, performance, and ergonomics [27]. The software can create a biomechanical model of the human skeleton with 82 segments connected by joints, for a total of 162 degrees of freedom. Design techniques are exploited to simulate biomechanically possible, ergonomically reliable, and collision-free movements of human models [28].

Figure 1 Lateral view of the 95th percentile male dummy with the global reference system (xyz).

IPS IMMA software offers four main advantages: (i) the comfort function of the manikin allows a realistic posture prediction by minimizing the biomechanical load; (ii) the ability of automatically adapting the movement strategy to the performed activity makes the dummy adaptive; (iii) the possibility of building a personalized family of dummies with different anthropometric measures allows the execution of the simulation at the same time for the whole family; (iv) the simple interface allows a non-expert user evaluating the interaction between the human and the environment [28]. Additionally, IPS IMMA anthropometric module utilizes the Principal Component Analysis, and multivariate approach to generate dummies capturing the anthropometric diversity within a target population. The software exploits two main databases (IFPS 2007 and ANSUR 1989), with the possibility of adding anthropometric databases of specific populations [28,29]. Once the database is selected, the first step is represented by the definition of the dummy gender, weight, and height. Then, anthropometric measures of the dummy are defined based on the standard ISO 7250 – *Basic human body measurements for technological design*. Subsequently, the software allows to execute simulations of the desired movement, offering different tools for a real-time and complete biomechanical and ergonomic evaluation, i.e. the virtual integration of the human dummy with the environment, the assessment of segments length, and the evaluation of joints angles instant by instant.

2.2 SIMULATION

2.2.1 Creation of dummies

In the present study, the IPS IMMA software was exploited to create two dummies based on the Swedish IFPS database [30]. To represent most of the population of the database, a 95th percentile male dummy and a 5th percentile female dummy were selected. Accordingly, they represent the larger size and the smaller size individuals, respectively. Once the gender and the percentile were defined, the software derived through linear interpolation all the anthropometric measurements according to 7250 standards. The two dummies were positioned in the space with anatomical axes coinciding with the axes of a global reference system (xyz), as shown in Figure 1. Accordingly, the x-axis coincided with the anterior-posterior direction, the y-axis coincided with the medio-lateral direction, and the z-axis coincided with the vertical direction. The visible side on the screen was the left one for both the dummies. A model composed of the bike bottom bracket, the cranks, and the pedals was added. The cranks length was equal to 155 mm. Two attach points groups were defined: (i) the Driving Seat allowed the dummy to assume a seated position; (ii) the Driving Feet allowed the dummy feet to reach the cranks. In detail, the Driving Seat was rotated of 30 degrees clockwise on the sagittal plane and associated to the dummy. The Driving Feet was associated to the cranks, imposing a translation constraint of 10 mm along the three axes and infinite rotational freedom. Hence, the feet followed the rotational movements of the cranks.

2.2.2 Definition of dummies optimal posture

The following check points were identified in both dummies:

- Top of Head as the highest point of the head
- Right Shoulder Joint as the right shoulder centre
- Left Shoulder Joint as the left shoulder centre
- Right Hand as the centre of the right hand palm
- Left Hand as the centre of the left hand palm
- Right Hip as the centre of the right hip
- Left Hip as the centre of the left hip
- Right Knee as the centre of the right knee
- Left Knee as the centre of the left knee
- Right Ankle as the centre of the right ankle
- Left Ankle as the centre of the left ankle
- Right Toe Tip as the right toe point
- Left Toe Tip as the left toes point

Subsequently, four cubic graphical objects (20 x 20 x 20 mm) were created and positioned at the same medio-lateral coordinate (y-axis) in correspondence of specific dummies segments: Head, Gluteus, Knee, and Heel. Moreover, the Knee object was positioned in the same vertical coordinate (z-axis) of the Head object. The Heel object was positioned in the same vertical coordinate (z-axis) of the Head and Knee objects, and in the same anterior-posterior coordinate (x-axis) of the Gluteus object. Starting from these four graphical objects, three segments were defined (Head-Knee, Knee-Heel, and Heel-Gluteus) through the Linear Measurements tool, hence providing indications about the dummies' encumbrance on the sagittal plane.

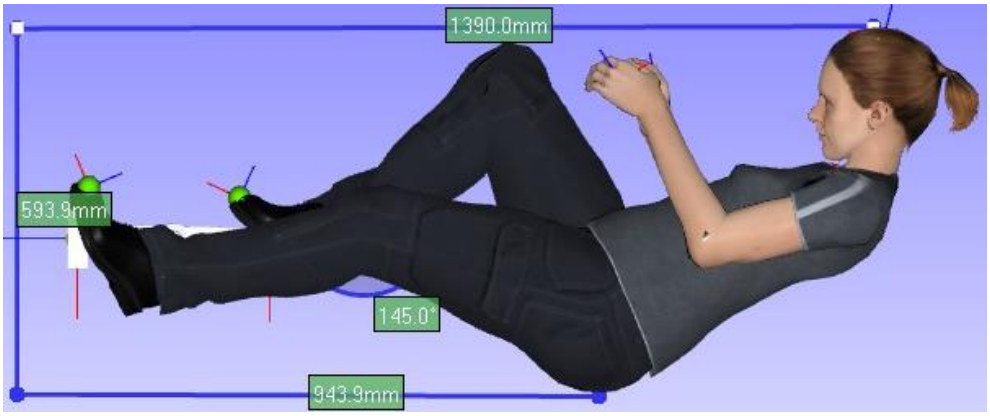

Figure 3 The 5th percentile female dummy with the encumbrance dimensions in the sagittal plane.

The tool Angular Measurements was used to define the flexion angle of the left knee as the angle between the two segments connecting the check points of Left Hip, Left Knee, and Left Ankle. Moving the Top of Head, Right Hand, Left Hand, and Driving Seat, the trunk of the dummies was inclined to reduce the frontal encumbrance of the cyclist as much as possible. In detail, the length of the segment between the Knee and the Heel was progressively reduced. Moreover, a particular attention was given to two positions of the crank, the Bottom Dead Centre (BDC) and the Top Dead Centre (TDC). In the case of a traditional bike, the BDC is the crank position when the leg is fully extended, whereas the TDC is the crank position when the foot is at the top of the pedal stroke [31]. If the bicycle is recumbent as in this study, the rider body is rotated of 90 degrees clockwise (Figure 2): the point in which the leg is fully extended occurs at the Anterior Dead Centre (ADC), whereas the point corresponding to the foot at the top of the pedal stroke occurs at the Posterior Dead Centre (PDC).

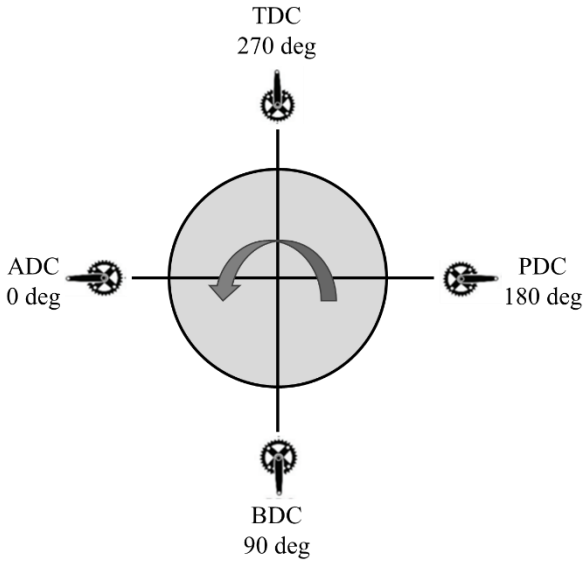

Figure 2 Pedalling cycle of a recumbent bicycle. The arrow identifies the counterclockwise rotation of the wheel.

In BDC, the segment between the Gluteus and the Heel was exploited to verify that the left heel of the dummy was not under the level of the gluteus along the vertical direction (z-axis). With a crank angle equal to 180 degrees, the segment between the Head and the Knee was used to verify that the left knee was not over the level of the head along the vertical direction (z-axis). Moreover, moving the cranks in the x-z plane, a flexion angle of 145 degrees was guaranteed in correspondence of a crank angle equal to 0 degrees. Finally, other two conditions were verified: (i) both knees did not overcome the segment defined by Head and Knee; (ii) both heels did not be below the Gluteus. Accordingly, the encumbrance of both dummies (Table I) was optimized (Figure 3). Actually, the only important segment for the encumbrance in the sagittal plane was the one from Knee to Heel, while the other two segments were just graphically derived.

Table I – Segments (mm) of encumbrance in the sagittal plane for both dummies

	95th percentile male	5th percentile female
Head-Knee	1275.9	943.9
Knee-Heel	608.0	593.9
Heel-Gluteus	1891.0	1390.0

2.2.3 Execution of simulation and data analysis

Once the optimal posture was reached, the Angular Measurements tool was also exploited to visualize the flexion angles of dummies hip, knee, and ankle from the segments formed by the corresponding check points. To evaluate the inclination of the trunk with respect to the vertical direction, a new graphical object was inserted with the same anterior-posterior (x-axis) and medio-lateral (y-axis) coordinates of the Left Hip check point. Then, the angle was defined as the angle between the segments formed by this object with the Left Hip and the Left Shoulder. Angles were evaluated as shown in Figure 4. The cranks were rotated counterclockwise starting from the left crank positioned at 0 degrees and hence the values of trunk, hip, knee, and ankle angles were saved every five degrees.

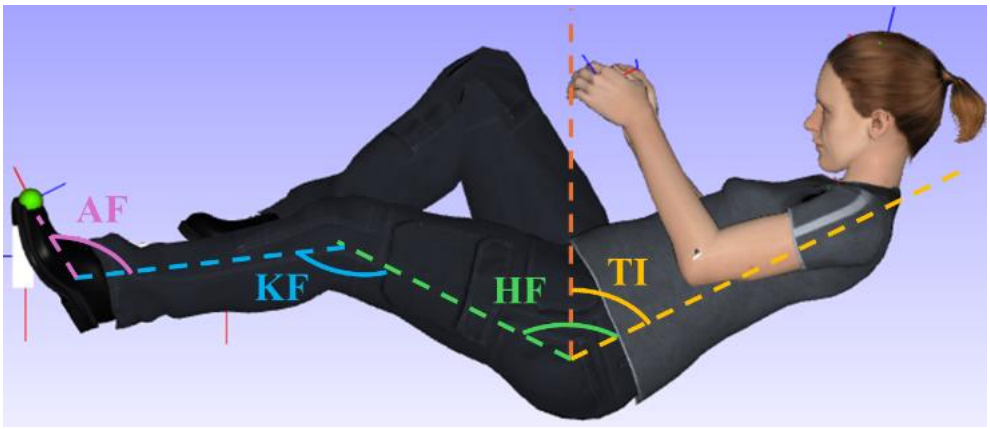

Figure 4 The estimated joint angles: the trunk inclination (TI) is formed by the trunk with respect to the vertical direction; the hip flexion (HF) is formed by the thigh with respect to the trunk; the knee flexion (KF) is formed by the shank with respect to the thigh; the ankle flexion (AF) is formed by the foot with respect to the shank.

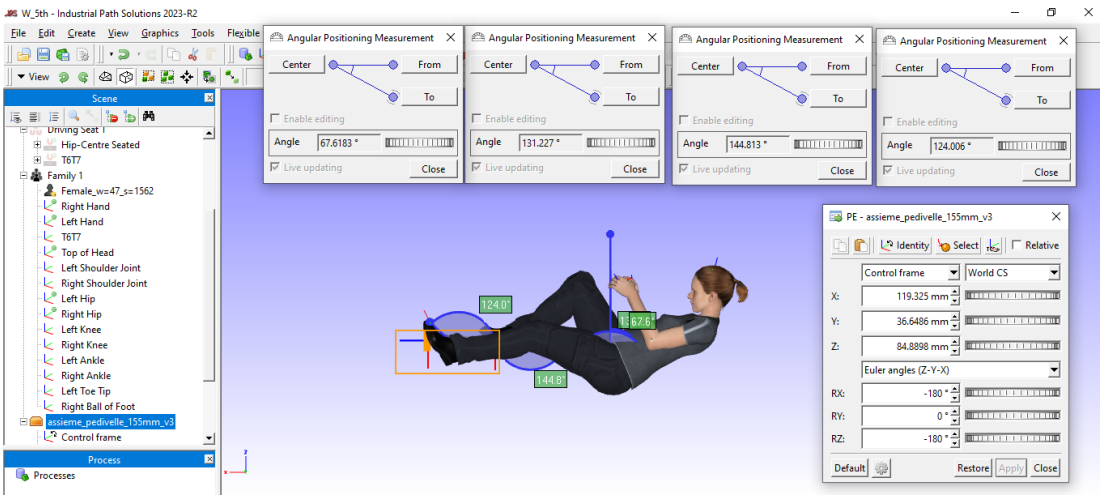

Figure 5 An exemplificative screen of IPS IMMA software functioning with the main available tools.

Since the software needs an ergonomic equilibrium, these values were saved after reaching a steady-state condition, i.e. after 3 complete rounds. During the simulation, Top of Head, Left Hand, Right Hand, Left Hip, and Right Hip points were blocked assuming them still. Figure 5 shows IPS IMMA software functioning.

3 RESULTS

Table II contains mean and standard deviation values of trunk, hip, knee, and ankle angles (deg). Table III contains ranges of motion (ROM) of hip, knee, and ankle angles (deg). These values were estimated for both the 95th percentile male and the 5th percentile female considering the whole fourth pedalling cycle of the simulation, which was selected as a steady-state condition. Trends of hip, knee, and ankle angles during the crank cycle are reported in Figures from 6 to 8 for both the 95th percentile male (blue curves) and the 5th percentile female (red curves). Asterisks composing these curves are related to angular values saved every 5 degrees of the fourth pedalling cycle. The vertical black dashed lines identify the key points of the pedalling cycle: 90 degrees = BDC, 180 degrees, and 270 degrees = TDC. Considering the crank angle values of 0, 90, 180, and 270 degrees, corresponding hip, knee, and ankle angles are reported in Tables from IV to VI from both the 95th percentile male and the 5th percentile female dummies. Finally, Table VII contains minimum hip and knee angles estimated over the whole pedalling cycle and their corresponding values of the crank angle.

Table II – Mean ± standard deviation joint angles (deg) estimated over the pedalling cycle

	95th percentile male	5th percentile female
Trunk inclination	72.5 ± 0.1	67.6 ± 0.0
Hip flexion	114.5 ± 15.1	109.7 ± 16.3
Knee flexion	109.7 ± 23.3	106.4 ± 26.1
Ankle flexion	132.2 ± 1.2	124.0 ± 2.2

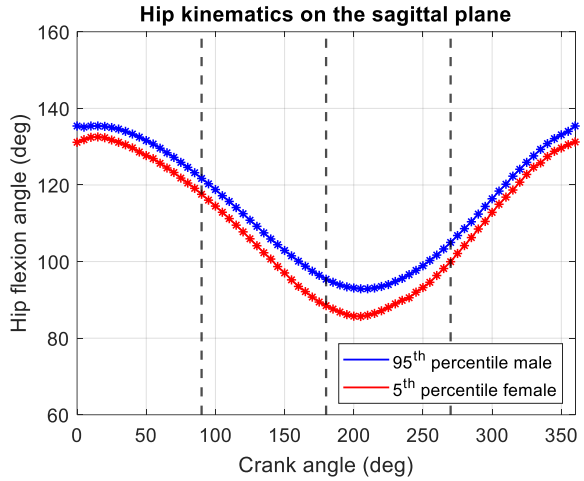

Figure 6 Hip flexion angle with respect to the crank angle for both dummies.

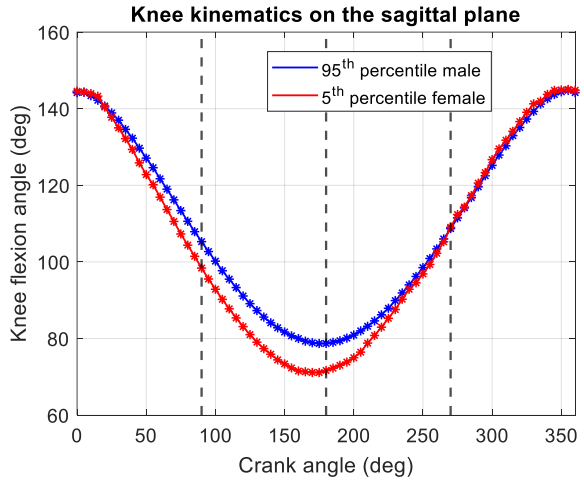

Figure 7 Knee flexion angle with respect to the crank angle for both dummies.

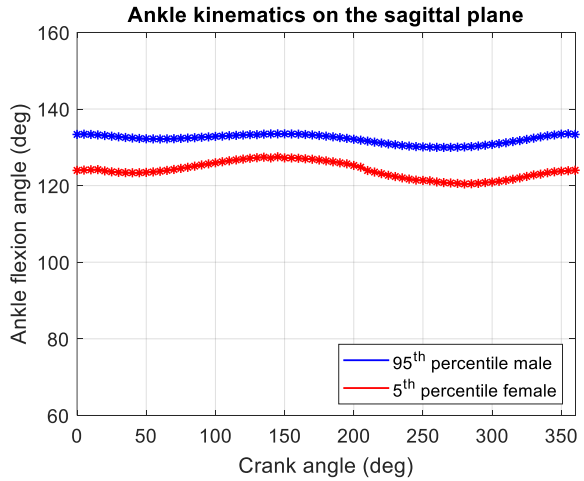

Figure 8 Ankle flexion angle with respect to the crank angle for both dummies.

Table III – ROM of joint angles (deg) estimated over the pedalling cycle

	95th percentile male	5th percentile female
Hip flexion	42.5	46.9
Knee flexion	66.1	73.9
Ankle flexion	3.6	7.1

Table IV – Hip flexion angles (deg) at specific values of the pedalling cycle

Crank angle (deg)	95th percentile male	5th percentile female
0	135.4	131.1
90	121.7	117.6
180	95.4	88.5
270	105.0	100.0

Table V – Knee flexion angles (deg) at specific values of the pedalling cycle

Crank angle (deg)	95th percentile male	5th percentile female
0	144.2	144.6
90	105.3	98.4
180	78.7	71.7
270	109.0	109.0

Table VI – Ankle flexion angles (deg) at specific values of the pedalling cycle

Crank angle (deg)	95th percentile male	5th percentile female
0	133.4	124.0
90	132.6	125.4
180	132.9	126.5
270	130.0	120.7

Table VII – Minimum hip and knee flexion angles (deg) and corresponding values of the crank angle

		Crank angle (deg)	Minimum angle (deg)
Hip	95th percentile male	205	92.9
	5th percentile female	205	85.7
Knee	95th percentile male	175	78.7
	5th percentile female	175	71.1

4 DISCUSSIONS

The aim of the present study was to exploit a computational method to prepare for the bicycle fitting of a recumbent bicycle, estimating the cyclist's encumbrance to optimize the performance. The angular trends of trunk, hip, knee, and ankle of both a 95th percentile male and a 5th percentile female were obtained in the sagittal plane during the pedalling cycle. The main imposed condition influencing all the posture and the encumbrance is the one on the knee flexion angle when the crank angle is equal to 0 degrees. This condition can be considered correct comparing the value

imposed with the software in the present work (145 degrees) with the one recommended in [17]. Since in this study the knee flexion angle was considered as the angle between the shank and the thigh segments while in [17] it was considered with respect to the extension of the thigh segment, the sum of the two values should be 180 degrees. Indeed, the present study imposed an angle equal to 145 degrees, while literature suggests an angle between 30 and 40 degrees. This aspect is confirmed in [18], which also estimates the knee flexion angle with respect to the extension of the thigh segment and hence, when the leg is fully extended, it recommends a range of the knee flexion angle between 30 and 40 degrees. This range adds up to 180 degrees with the angle imposed in the present simulation. This value allows preventing injuries while optimizing the cycling efficiency. Indeed, a greater knee flexion has a negative effect on the trunk comfort, provoking higher levels of fatigue and pain perception in the anterior part of the thigh and knee.

As Table II shows, the trunk inclination has very small standard deviation values because both the head and the hips were kept fixed during the pedalling gesture. Considering the mean values of trunk inclination, results are in line with literature. Indeed, Telli et al. estimated the torso angle as the one formed by the hip-shoulder segment and the horizontal line passing through the hip joint [9]. In the present study, the trunk inclination was estimated with respect to the vertical direction passing through the hip joint centre and hence it is almost complementary (between 68 and 73 degrees) to the one imposed by Telli et al. (around 30 degrees). Considering the mean values of hip and heels (Table II), the values provided by the software (around 115 degrees for the hip and 110 degrees for the knee) are in line with previous results found in literature [11].

As shown in Table III, the same consideration can be made for hip and knee ROM (around 45 degrees for the hip and 70 degrees for the knee), which are similar to the ones reported in the study of Kato et al. (around 50 degrees for the hip and 80 degrees for the knee) [11] and the one of Trumbower et al. (around 40 degrees for the hip and 60 degrees for the knee) [16]. Considering the mean values of ankle angle reported in Table II (around 130 degrees), it is similar to one found by Holliday et al. (around 110 degrees) [32], but the gap between the two results can be due to the different inclination of the bicycle (traditional vs recumbent). Moreover, both the small standard deviation values (between 1 and 2 degrees) reported in Table II and the small ROM (from 3 to 7 degrees) reported in Table III of the ankle angle are in line with literature, especially considering the ROM values provided in [16].

Focusing on the hip angular trend reported in Figure 6, it starts with a value of around 135 degrees in correspondence of a crank angle of 0 degrees. Then, the value decreases until reaching a flexion peak occurring at a crank angle of around 205 degrees for both dummies (Table VII). This peak occurs after 180 degrees because of the recumbent configuration of the bike, which inclines the trunk axis of around 20 degrees with respect to the horizontal direction. After this flexion peak, the angle increases again until the initial value. Considering the angular trend of the knee (Figure 7), the imposed initial value is around 145 degrees. Subsequently, there is a flexion peak occurring at a crank angle of around 180 degrees for both dummies (Table VII) and then the angle rises again. The flexion of the ankle (Figure 8) slightly oscillates around a mean value of 130 degrees (Table II).

Even if the angular trends are the same for both dummies, the 95th percentile male is characterized by values of joint angles greater (of around 5%) than the 5th percentile female ones. Considering the hip and the knee, this difference is more appreciable around a crank angle of 180 degrees. This aspect can be justified considering that the crank length is the same for both dummies, whereas the male has a longer leg than the female. Accordingly, the female is forced to flex the knee more than the male and hence female ROM are greater than male ones (of at least 10%).

5 CONCLUSIONS

Overall, results provided by the present study confirm the suitability of computational methods in the process of bike fitting. In detail, the IPS IMMA software represents a useful tool to estimate the cyclist's encumbrance in both the sagittal and the frontal plane, to evaluate the joint angular trends during the pedalling cycle, and hence to optimize the performance. By analysing the angular trends of the trunk, hip, knee, and ankle in both a 95th percentile male and a 5th percentile female during the pedalling cycle, insights were gained into the optimal positioning required to prevent injuries and optimize cycling efficiency. The study confirmed that maintaining a knee flexion angle within the recommended range of 30 to 40 degrees (or around 145 degrees if calculated with respect to the thigh segment and not with respect to its extension) is crucial for preventing injuries while optimizing cycling efficiency. Additionally, trunk inclination and joint ranges of motion were found to be consistent with previous literature, indicating the validity of the computational methodology. The study also highlighted differences between the male and female dummies, with the male exhibiting greater joint angles due to differences in their height and hence in their leg length. Overall, the findings contribute to our understanding of optimal bicycle fitting and provide valuable insights for designing recumbent bicycles that optimize both performance and comfort for cyclists of varying anthropometric characteristics.

ACKNOWLEDGEMENTS

The authors thank the Policumbent Student Team for providing the test case and the Biomedical Division of the team for assisting in the numerical simulations performance. Moreover, the authors extend their sincere gratitude to Valerio Cibrario, Director of fleXstructures Italia, for generously providing the IPS IMMA license and invaluable support.

REFERENCES

[1] Yen, C. C., Wei, W. L., and Tao, L., Cycling Comfort Levels for Recumbent Exercise Bicycles. Applied Mechanics and Materials, Vol. 423, pp. 1847-1852, 2013.

[2] Digo, E., Gastaldi, L., Antonelli, M., Cornagliotto, V., and Pastorelli, S., Estimation of force effectiveness and symmetry during kranking training. *Quaglia, G., Gasparetto, A., Petuya, V., Carbone, G. (eds) Proceedings of I4SDG Workshop 2021. I4SDG 2021. Mechanisms and Machine Science*, Vol. 108, pp. 201-208, 2022.

[3] Rose, G., and Liang, A., Velomobiles and Urban Mobility: Opportunities and Challenges. Small Electric Vehicles: An International View on Light Three- and Four-Wheelers, pp. 29-39, 2021.

[4] Jongerius, N., Wainwright, B., Walker, J., and Bissas, A., The Biomechanics of Maintaining Effective Force Application across Cycling Positions. Journal of Biomechanics, Vol. 138, 2022.

[5] Baldissera, P., and Delprete, C., External and Internal CFD Analysis of a High-Speed Human Powered Vehicle. International Journal of Mechanics and Control, Vol. 17, No. 2, pp. 27-34, 2016.

[6] Swart, J., and Holliday, W., Cycling Biomechanics Optimization-the (R) Evolution of Bicycle Fitting. Current Sports Medicine Reports, Vol. 18, No. 12, pp. 490-496, 2019.

[7] Millour, G., Velásquez, A. T., and Domingue, F., A Literature Overview of Modern Biomechanical-Based Technologies for Bike-Fitting Professionals and Coaches. International Journal of Sports Science and Coaching, Vol. 18, No. 1, pp. 292-303, 2023.

[8] Silberman, M. R., Webner, D., Collina, S., and Shiple, B. J., Road Bicycle Fit. Clinical Journal of Sport Medicine, Vol. 15, No. 4, pp. 271-276, 2005.

[9] Telli, R., Seminati, E., Pavei, G., and Minetti, A. E., Recumbent vs. Upright Bicycles: 3D Trajectory of Body Centre of Mass, Limb Mechanical Work, and Operative Range of Propulsive Muscles. Journal of Sports Sciences, Vol. 35, No. 5, pp. 491-499, 2017.

[10] Wehrle, A., Waibel, S., Gollhofer, A., and Roecker, K., Power Output and Efficiency During Supine, Recumbent, and Upright Cycle Ergometry. Frontiers in Sports and Active Living, Vol. 3, 2021.

[11] Kato, M., Tsutsumi, T., Yamaguchi, T., Kurakane, S., and Chang, H., Characteristics of Maximum Performance of Pedaling Exercise in Recumbent and Supine Positions. Journal of Sports Science and Medicine, Vol. 10, No. 3, p. 491, 2011.

[12] Scoz, R. D., Amorim, C. F., Espindola, T., Santiago, M., Mendes, J. J. B., De Oliveira, P. R., Ferreira, L. M. A., and Brito, R. N., Discomfort, Pain and Fatigue Levels of 160 Cyclists after a Kinematic Bike-Fitting Method: An Experimental Study. BMJ Open Sport and Exercise Medicine, Vol. 7, No. 3, 2021.

[13] Thorsen, T., Strohacker, K., Weinhandl, J. T., and Zhang, S., Increased Q-Factor Increases Frontal-Plane Knee Joint Loading in Stationary Cycling. Journal of Sport and Health Science, Vol. 9, No. 3, pp. 258–264, 2020.

[14] Lu, T., Thorsen, T., Porter, J. M., Weinhandl, J. T., and Zhang, S., Can Changes of Workrate and Seat Position Affect Frontal and Sagittal Plane Knee Biomechanics in Recumbent Cycling?. Sports Biomechanics, Vol. 22, No. 4, pp. 494–509, 2023.

[15] Momeni, K., Faghri, P. D., and Evans, M., Lower-Extremity Joint Kinematics and Muscle Activations during Semi-Reclined Cycling at Different Workloads in Healthy Individuals. Journal of Neuroengineering and Rehabilitation, Vol. 11, No. 1, 2014.

[16] Trumbower, R. D., and Faghri, P. D., Kinematic Analyses of Semireclined Leg Cycling in Able-Bodied and Spinal Cord Injured Individuals. Spinal Cord, Vol. 43, No. 9, pp. 543–549, 2005.

[17] Priego Quesada, J. I., Pérez-Soriano, P., Lucas-Cuevas, A. G., Salvador Palmer, R., and Cibrián Ortiz de Anda, R. M., Effect of Bike-Fit in the Perception of Comfort, Fatigue and Pain. Journal of Sports Sciences, Vol. 35, No. 14, pp. 1459–1465, 2017.

[18] Ferrer-Roca, V., Roig, A., Galilea, P., and GarcíA-Lopez, J., Influence of Saddle Height on Lower Limb Kinematics in Well-Trained Cyclists: Static vs. Dynamic Evaluation in Bike Fitting. Journal of Strength and Conditioning Research, Vol. 26, No. 11, pp. 3025–3029, 2012.

[19] Van Hoof, W., Volkaerts, K., O'sullivan, K., Verschueren, S., and Dankaerts, W., Comparing Lower Lumbar Kinematics in Cyclists with Low Back Pain (Flexion Pattern) versus Asymptomatic Controls e Field Study Using a Wireless Posture Monitoring System. Manual therapy, Vol. 17, No. 4, pp. 312-317, 2012.

[20] Baldissera, P., Delprete, C., and Tirelli, M., Velomobiles: Design Guidelines. International Journal of Mechanics and Control, Vol. 13, No. 2, pp. 41–49, 2023.

[21] Baldissera, P., and Delprete, C., Rolling Resistance, Vertical Load and Optimal Number of Wheels in Human-Powered Vehicle Design. *Proc. of the Institution of Mechanical Engineers, Part P: Journal of Sports Engineering and Technology*, Vol. 231, No. 1, pp. 33–42, 2016.

[22] Vella, A. D., Lisitano, D., Tota, A., and Wang, B., Analysis of Heavy Commercial Vehicle Cornering Behaviour through a Multibody Model. International Journal of Mechanics and Control, Vol. 21, No. 2, pp. 39–50, 2022.

[23] Vella, A. D., Digo, E., and Vigliani, A., Experimental Analysis and Multibody Simulation of Electric Kick Scooter Braking Maneuver. *Okada, M. (eds) Advances in Mechanism and Machine Science. IFToMM WC 2023. Mechanisms and Machine Science*, Springer, Cham, Vol. 149, pp. 533-540, 2024.

[24] Panero, E., Muscolo, G. G., Gastaldi, L., and Pastorelli, S., Multibody analysis of a 3D human model with trunk exoskeleton for industrial applications. *Proc. of the 9th ECCOMAS thematic conference on multibody dynamics*, pp. 43-51, 2020.

[25] Korytov, M. S., Shcherbakov, V. S., and Kashapova, I. E., Investigation of Dynamic Characteristics of the Vibration Isolation System for Operators' Seat. International Journal of Mechanics and Control, Vol. 24, No. 2, pp. 19–38, 2023.

[26] IPS | Industrial Path Solutions | Industrial Path Solutions, https://industrialpathsolutions.se/#top.

[27] Krochman, A., and Kuebler, T., Cognitive Analysis of Multiscreen Passenger Vehicles. Human-Automation Interaction. Automation, Collaboration, & E-Services, Vol. 11, pp. 147–155, 2023.

[28] Brolin, E., Högberg, D., and Hanson, L., Design of a Digital Human Modelling Module for Consideration of Anthropometric Diversity. *Proc. of the 5th AHFE Conference*, Jagiellonian University, 2014.

[29] Brolin, E., Hanson, L., Högberg, D., Rhen, I.-M., Bertilsson, E., Hanson, L., Högberg, D., and Rhén, I. M., Creation of the IMMA Manikin with Consideration of Anthropometric Diversity. *Proc. the 21st International Conference on Production Research (ICPR)*, pp. 416–420, 2014.

[30] Hanson, L., Sperling, L., Gard, G., Ipsen, S., and Olivares Vergara, C., Swedish Anthropometrics for Product and Workplace Design. Applied Ergonomics, Vol. 40, No. 4, pp. 797–806, 2009.

[31] Wadsworth, D. J., & Weinrauch, P., The role of a bike fit in cyclists with hip pain. a clinical commentary. International Journal of Sports Physical Therapy, Vol. 14, No. 3, p. 468, 2019.

[32] Holliday, W., Fisher, J., Theo, R., and Swart, J., Static versus Dynamic Kinematics in Cyclists: A Comparison of Goniometer, Inclinometer and 3D Motion Capture. European Journal of Sport Science, Vol. 17, No. 9, pp. 1129-1142, 2017.